Chapter

Electromagnetism of Microwave Heating

Rafael Zamorano Ulloa

Abstract

Detailed electrodynamic descriptions of the fundamental workings of microwave heating devices are presented. We stress that all results come from Maxwell equations and the boundary conditions (BC). We analyze one by one the principal components of a microwave heater; the cooking chamber, the waveguide, and the microwave sources, either klystron or magnetron. The boundary conditions at the walls of the resonant cavity and at the interface air/surface of the food are given and show how relevant the BC are to understand how the microwaves penetrate the nonconducting, electric polarizable specimen. We mention the application of microwaving waste plastics to obtain a good H_2 quantity that could be used as a clean energy source for other machines. We obtained trapped stationary microwaves in the resonant cavity and traveling waves in the waveguides. We show 3D plots of the mathematical solutions and agree quite well with experimental measurements of hot/cold patterns. Simulations for cylindrical cavities are shown. The radiation processes in klystrons and magnetrons are described with some detail in terms of the accelerated electrons and their trajectories. These fields are sent to the waveguides and feed the cooking chamber. Whence, we understand how a meal or waste plastic, or an industrial sample is microwave heated.

Keywords: microwave heating, resonant cavity, cooking chamber, waveguide, klystron, magnetron, boundary conditions, food-air interface, Lienard-Wiechert potentials, Jefimenko fields

1. Introduction

Microwaves are everywhere and permeate the universe. They reach earth constantly and we produce them in many medical, industrial, chemical, domestic, and research on magnetic and dielectric materials and in devices and equipment [1–13]. The modern communications technology uses them intensely, Wi-Fi, all around the world, every second, every day [14]. Many medical applications are concentrated in cancer treatments by giving hyperthermia to the cancerous cells while avoiding to damage healthy cells. Microwave ablation is widely used in many types of cancers, bone, cardiac arrhythmic tissue, thyroid glands, skin cancer, and many other damaged tissues [2, 3, 15, 16]. The apparatus is constituted basically by a microwave source, a waveguide that ends in an antenna that, as a needle, penetrates the tissue [2, 3, 15, 16]. Industrial applications go from thermally treating/curing polymers, rubber, and plastics to quickly heat cement and minerals, and to assist vulcanization [4, 5, 17, 18]. Chemical applications are mainly directed to organic and/or inorganic synthesis and accelerating reactions, and to search for novel synthesis routes and

novel products. Chemical microwave heating has been used for decades [6, 7]. Research in magnetics and in dielectrics includes heat transfer and/or electromagnetic excitation of matter [10–13]. Domestic technology uses them to heat up quickly and easily food, coffee, and water in microwave ovens (MWO) built for such function, see **Figure 1(D)** [8, 9]. By far, the two most commonly used microwave configurations include a source of microwaves, typically a klystron or a magnetron, a waveguide for these microwaves, and a resonant chamber where the microwaves are used to treat, to modify, to cure, to excite, or to heat up a sample put in the microwave chamber. There are two most common geometries of microwave chambers, cylindrical and rectangular [4–13]. **Figure 1(A)** shows an electric field pattern simulated inside a typical cylindrical cavity (3.4 cm of radius and 4.22 cm of height) used in a research equipment, in which magnetic samples are resonantly excited [19]. The magnetic field (not shown) is vertical (and orthogonal to E) and mostly concentrated along the z-axis at $r = 0$ and to its close vicinity. **Figure 1(B)** shows an electron paramagnetic resonance spectrometer that uses a cylindrical microwave chamber feed by a rectangular waveguide that collects the 9.4-GHz low-power microwaves produced by a klystron inside the box-labeled microwave bridge. **Figure 1(C)** is a calculated stationary electric field pattern from the solutions to Maxwell equations found in this work for a rectangular cavity. **Figure 1(D)** shows a typical domestic microwave oven of dimensions 26 cm × 30 cm × 34 cm.

A universal advantage of microwave heating in industrial, medical, chemical, and domestic processes is that it does it quickly and efficiently. Yet, several investigations are pursued to find even faster and better microwave heating schemes and profiles [15–17].

The three main parts of these heating devices constitute a source, a waveguide, and a heating chamber. **Figure 2(A)** shows the essential parts of a microwave oven commonly used to heat food. In addition to the already large number of industrial microwave heating applications, very recently, microwaving plastic waste decomposition has been proposed as a central step in order to generate clean hydrogen, H_2, out of heating a one-to-one mixture of triturated waste plastics with the catalyst FeAlOx [20]. Edwards et al. [21] have used microwaves to transform waste plastic bags, milk empty bottles, and other supermarket waste plastics, **Figure 2(B)**, in a clean hydrogen energy source. A 1:1 mixture of the catalyst FeAlOx and waste plastics heated up with microwaves in a cylindrical cavity

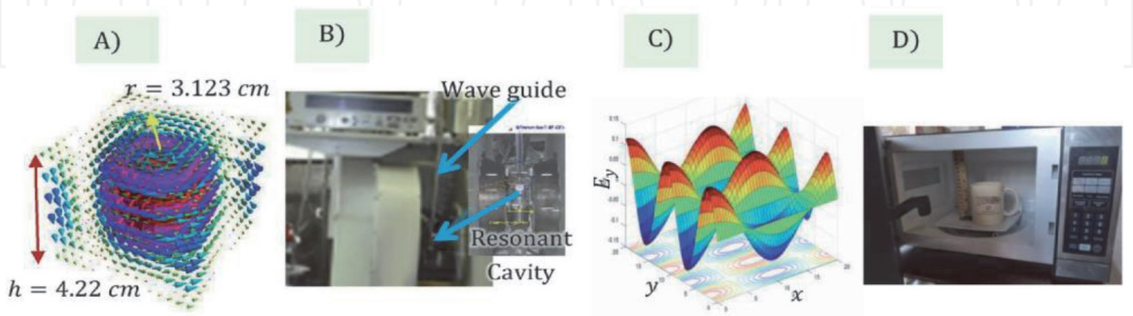

Figure 1.
Microwaves in cylindrical and rectangular geometries. (A) Simulation of the electric field, circular, pattern formed inside a cylindrical microwave cavity. (B) The microwave bridge, the rectangular waveguide, and a cylindrical cavity of a commercial electron paramagnetic resonance spectrometer used to excite magnetic samples. Here, heating is not desired, and the microwave power used is 1 mW or less. (C) A stationary electric field pattern calculated in this work from the solutions to Maxwell equations. The pattern is calculated for the planes x *and* y *with the coordinate* z *maintained fixed at an arbitrary height. (D) A typical domestic microwave oven (MWO), open and showing its internal chamber height* h = *38 cm, and width* a = *32 cm and* b = *depth, 30 cm.*

Figure 2.
Microwave heating. (A) A typical 1000 Watts, 2.45-GHz domestic microwave oven (MWO) cooking a chicken. (B) Plastic pollution derived from tons and tons of waste plastic bottles and supermarket bags. (C) Clean production of H_2 by microwaving waste plastic bags and bottles mixed 1:1 with the catalyst FeAlOx within a cylindrical cavity, the input power is 1000 Watts, and H_2 gas is liberated and carried toward a separate container. The cylindrical cavity operates in the TM_{010} mode.

(as shown in **Figure 2(C)**) for 10, 30, and 60 s extracts 85–90% of molecular hydrogen that is sent through a column to be stored in a separate chamber for its eventual utilization as a clean energy source. The principle of operation is the same for the domestic microwave oven with a rectangular heating chamber and for this microwave heater that is used to transform waste plastics within a cylindrical heating chamber. This transformation process is clean and fast and could help to reduce drastically the world's wide plastic contamination problem. Plastics invade mountains [22], forests, lakes, oceans, and cities [20–22]. As the hydrogen density content in plastic bags is around 14% per weight, its transformation into H_2 and multifaceted fullerenes might offer an opportunity of clean energy production for the countries interested in producing clean H_2 as a viable energy source for industrial and domestic usage and contribute to slowing down the global climate change [23]. Using tons and tons of garbage plastics, H_2 can be produced in high quantities and then used as a clean industry and house energy supply, this way contributing to combat the global warming. We consider this kind of potential application relevant for the plastic industry and pollution problems and much more relevant for its contribution to a cleaner, greener planet. Microwave heating is used globally, also, to cook or just heat up meals, water, coffee, and pizza. These microwave ovens operate at a power of 1000 Watts; the meals are put into a rectangular resonant cavity that is the cooking chamber that gives them their familiar "box" appearance. In this box, microwaves are delivered unevenly (see uneven electric field pattern calculated here and shown in **Figure 1(C)**), to the meals, and they readily penetrate the matter, making electric dipoles (mainly from water and fatty molecules) to oscillate frenetically; then, this excitation energy is passed to the rest of the specimen as heat.

In a few seconds or minutes, the specimen is hotter than at the start of the microwaving [5–13]. The utility of microwaves is multiple and of large range. In spite of the generalized use of microwave ovens, an informal survey has indicated to us that more than 90% of our STEM students do not really know how MWOs operate. The basic physics required to understand their workings is completed by the end of the undergraduate class work. This is telling us the degree of sophistication and depth that this technology carries, just as many other modern technologies do, as the Wi-Fi itself. A primal objective of this chapter is to describe its electromagnetic physics and to give the fundamentals. All comes from Maxwell equations. We emphasize the fact that most of the microwave heating devices (as the two devices shown in **Figure 2**) are composed of three essential electromagnetic parts: the production of the microwaves, their wave-guided structure that brings the

microwaves from their origins toward the resonant cavity, being the third essential component, that is, the cooking chamber. Aforesaid, some devices use rectangular resonant cavities and others use cylindrical resonant cavities. We focus on rectangular cavities and just mention some results for cylindrical cavities.

We want to emphasize that the study of the electromagnetic functioning of a domestic, an industrial, or a laboratory MWO is an ideal technological case to see how the whole of the theory is applied. These microwave "boxes" contain all of the fundamental physics required to produce (in klystrons or magnetrons) microwaves, then input them into a loss-less waveguide, and finally get them to bath a rectangular heating chamber, or a cylindrical chamber, without appreciable microwave radiation being absorbed at the metallic walls. Their absorption is mainly carried out, precisely, by the specimen we want to heat up.

Our discussion has five parts: First, in Section 2, we deal qualitatively, in detail, with the fundamental constituents of a microwave heating system and the physical processes involved. Then, in Section 3, we analyze the boundary conditions, and in Section 4, we treat mathematically the resonant cavity. A description of the physics of this resonant cavity that keeps confined the microwaves all the time necessary for the food to warm up, or even be cooked, is given. We show that standing wave patterns are the solutions to Maxwell equations. Section 5 treats the rectangular waveguide and the general form of the traveling waves in them is obtained. The process of wave guiding the microwaves is the one that carries the microwaves from its source to the heating chamber. Then, in Section 7, we treat the production of microwaves in klystrons and/or magnetrons by radiating, accelerated, electrons moving in straight lines, or curved trajectories.

2. Fundamental constituents of a microwave heater

In formal terms, a domestic microwave oven [8, 9], or an industrial system [4, 5] or a laboratory prototype for clean extraction of H_2 from microwaving waste plastics [20, 21], is constituted by three fundamental parts shown in **Figure 2(A)** and **(C)** and in **Figure 3**.

(A) The resonant cavity: Once the microwaves are inside the rectangular cooking chamber, **Figure 2(A)**, or inside a cylindrical resonant cavity, **Figure 2(C)**, these microwaves display themselves stationary wave patterns since they are confined within good conducting walls, see **Figure 1(A)** and **(C)**. These waves rebound incessantly from these metallic walls without, practically, any energy loss. These wave patterns are specific for each geometry and each set of dimensions and the boundary conditions at the walls, as we show below.

In MWOs, the sixth wall is the see-through door that allows access to the interior of the chamber. The see-through window is covered by a metallic mesh with many

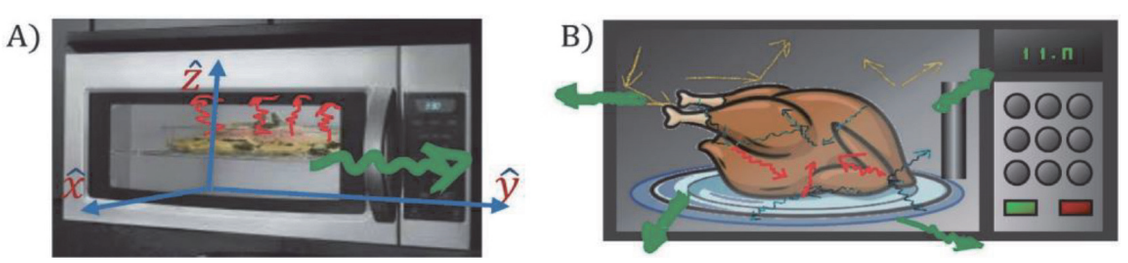

Figure 3.
Food being cooked in a microwave oven. (A) The meal is already hot and steam is actually getting out of the meat, and the green wavy arrow is pointing to the possibility that some microwaves get out of the oven. (B) The microwaves rebound from all six metallic surfaces of the "box" (yellow) and are reflected and transmitted from the surface of the specimen been heated (blue and red).

small holes of $r \approx 1$ mm radius that does not allow microwaves to escape; the condition $\lambda >> r$ holds and, hence, it functions as a continuous metallic, highly reflecting, surface. The receptacle we see when we introduce the meal to be microwaved is the resonant cavity as shown in **Figure 3**. Electromagnetically, a rectangular resonant cavity, beneath the plastic covers, conforms to a metallic box of about $30 \times 32 \times 38$ cm^3 dimensions. A 3D standing wave pattern is self-established due to the boundary conditions that have to be fulfilled at the walls, see **Figure 1(C)**.

Hence, maxima and minima and zeroes of the electric field $\left(\vec{E}\right)$ and magnetic field $\left(\vec{B}\right)$ appear at different locations, x, y, z, inside the cooking chamber. These microwaves bouncing continuously from the six walls bath constantly and heat our meal.

Can the microwaves, green wavy arrows in **Figure 3**, escape from the cooking chamber? Not in principle, unless some malalignment, or broken piece is there. Within the resonant cavity, the microwaves bounce back and forth from the metallic walls (yellow in **Figure 3(B)**) without any loss of electromagnetic energy.

Then, the microwaves hit the chicken at multiple points (blue-green wavy arrows), at the interface between food and air, reflection and refraction take place, and Snell's law and Fresnel equations have to be fulfilled [24–29]. Some microwaves are reflected (blue-green lines), and others are transmitted inside the chicken body (red wavy arrows). These red microwaves are responsible for heating, and they are the ones that transmit, quite efficiently, vertiginous motions vibrations, at 2.45 GHz, to the electric dipoles that are part of the meal (mostly water, but also some fatty molecules). These red microwaves penetrate several centimeters through the specimen. The electromagnetic energy carried out by the Poynting vector of these red microwaves, $\vec{S}(r,t) = \vec{E}(r,t) \times \vec{H}(r,t)$, is converted into frenetic Jiggling of these polar molecules and then converted into heat by their interactions with surrounding, neighboring molecules. Heat can be so high that some steam (water vapor) can be seen through the window in just a few seconds, see **Figure 3 (A)**. This process is the moment of energy conversion: from electromagnetic energy with 1000 Watts of power to motion, vibrations, mechanical energy. But that excited motion starts, rapidly, to pass to neighboring nonpolar atoms and molecules and locally, all the surrounding matter, starts jiggling more and more, which is heat. *Microwave energy has been transformed into heat inside our meal being microwaved*. In **Figure 3**, the wavy red lines represent the microwaves that get into the specimen and excite the electric dipoles within it. We show that at multiple points of incidence-reflection-transmission on the food-air interface, this bathing is by no means uniform since the microwaves distribute inhomogeneously inside the resonant cavity, see **Figure 1(C)**. This is the reason why the specimen is placed on a rotating plate, so some homogeneous heating is achieved.

Normally, it is expected that the ceramic (or the plastic), from which the cup for coffee or water is made, does not get heated while the liquid inside it. In order to get such result, it is necessary to minimize the composition of electric dipoles in the structure of the ceramics, glass, or plastic that makes the cup or the dish, effectively rendering this object transparent to the microwaves.

(B) The metallic waveguide: The microwave radiation from the source is immediately channeled through a horn-like metallic collector toward a rectangular waveguide through multiple reflections on its conducting metallic walls, and the radiation is guided almost without attenuation to the resonant cavity of the MWO. A rectangular waveguide is shown in **Figures 1(B)** and **4(C)**. The good conductor quality of the waveguide is the responsible for no-attenuation microwaves at the

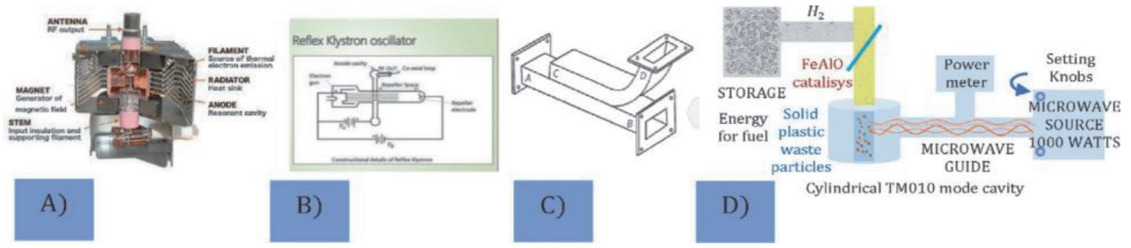

Figure 4.
Constituent parts of a microwave oven, or a laboratory microwave heater. (A) A magnetron typically used to generate microwaves in a domestic MWO. (B) A microwave generator, klystron, that is frequently used in microwave laboratory equipment where low power is required. (C) A hollow rectangular waveguide of a, b cross section and coupled to another waveguide, of the same dimensions, from aforesaid (taken from Feynman Phys. Lectures, vol. II. [24]) both microwave trains join and interfere at the union of the metallic structures. (D) An example of microwaving solids and trapping gasses that are detached, from the specimen, in the process. Microwaving plastic waste mixed 1:1 with FeAlOx inside the transformation chamber, which is an aluminum TM_{010} resonant cavity (it is the analog of the microwave oven chamber). Principle of operation was modified from [21], not the actual experimental setup.

waveguide walls even after multiple reflections. More detail on waveguides can be found in Refs. [24-29]. The waveguide terminates in a "mouth" that connects with the cooking chamber. This way both parts are coupled.

(C) The source of microwaves: For low-power applications, 1 mW or less, a klystron is used as the source of microwaves. For higher-power applications of microwave heating, around 1000 Watts, a magnetron is used. In both cases, it is a tube in which electrons are ejected from a hot cathode to a space where they get immediately accelerated and precisely, this acceleration produces electric and magnetic radiation fields, orthogonal to each other and to the propagation direction. Its power is proportional to the acceleration squared, Prad $\alpha\, a^2$, and is schematically depicted in **Figure 4(A)** and **(B)**. Those accelerated electrons emit radiation at the same frequency of the acceleration that in this case is in the 2–3 GHz range.

Now let us be more quantitative. We start with the electromagnetic boundary conditions.

3. Microwave heating of food or of an industrial sample

When microwave radiation hits the surface of a specimen, what we have is incidence of electromagnetic fields on the interface between meal and air, two nonmagnetic, nonconducting media, and the laws of Snell and Fresnel of reflection and refraction have to be fulfilled. But, they will be obeyed once the boundary conditions for $\vec{E}$ and $\vec{D}$ and for $\vec{H}$ and $\vec{B}$ are fulfilled. Let us see what they are as follows:

3.1 Continuity of the normal component of the displacement field, *D*

Let us suppose we have the interface between any two media such as water-air, plastic-metal, raw meat-hot air, a catalyst-plastic, ceramic-coffee, and so on as shown in **Figure 5**, that is, the boundary. The boundary condition on $\vec{D}$ is obtained from applying Gauss law to a very small cylinder (purple) of differential area and differential high that crosses the boundary as shown in **Figure 5(A)**. Then, the Gauss integral $\oint \vec{E} \cdot \vec{n} da$ on the closed surface is decomposed into three integrals, one on S_1 within medium 1, another one on surface S_2 within medium 2, and a third integral on the lateral surface, which goes to zero because the high of the cylinder is as small as we wish; then after integrating the only two integrals we are left with

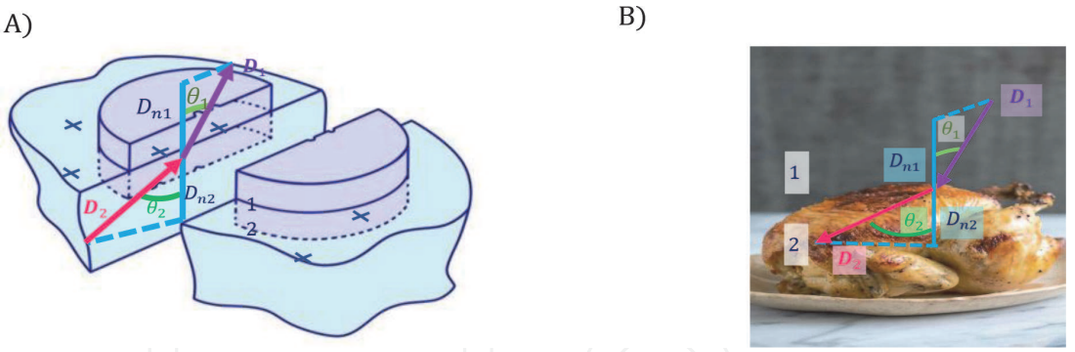

Figure 5.

Boundary conditions on $\vec{D}$. (A) Gaussian, very small, cylinder on the interface between two different media 1 and 2. The difference $D_{n1} - D_{n2}$ between the normal components of $\vec{D}$ is equal to the surface charge density σ_f. When surface charge is zero, then $D_{n1} = D_{n2}$, the normal components of the displacement field are continuous. (B) The same condition applies on the surface of meat when field $\vec{D}$ hits its surface inside a microwave oven, in this case $\sigma_f = 0$ and $D_{n1} = D_{n2}$. In (B) the boundary interface is the skin of a chicken being microwaved.

produce $(D_{n1} - D_{n2})S = \sigma_f S$ [25–29]. When the interface carries no electric charge, as is usually the case with microwave heating, then $\sigma_f = 0$. Hence, $(D_{n1} = D_{n2})$. And so, the normal component of the displacement vector is continuous through the interface of air-chicken!, or air-plastic, or air-ceramic, and so on.

Only in the case of the boundary between a conductor and a dielectric $D_n = \sigma_f$, being σ_f the free charge density on the interface as represented with the "+" signs in **Figure 5(A)**. For the cases we are interested here, all the metallic walls in the cooking chamber (resonant cavity) and the waveguide are not charged, then $\sigma_f = 0$ and so $D_{n1} = D_{n2}$.

On the other hand, when the $\vec{D}$, field of the microwaves in the cooking chamber enters the surface, D_{n2}, of the piece of food (sample, specimen, system), as shown in **Figure 5(B)**, it travels much more distance inside (several centimeters.) the sample and in its way excites electric dipoles (mostly water molecules and fat dipolar and other organic dipolar moieties) and gradually, but fast, transfers most of its energy to them. After a relaxation time period, $\approx 10^{-6}$ sec, the dipoles transfer all that juggling energy to vibrations of the bulk and appear as heat (measured as $k_B T$).

3.2 Continuity of the tangential component of the electric field intensity

Consider the blue, rectangular, path shown in **Figure 6(A)** and **(B)** with two sides parallel to the boundary and arbitrarily close to it. The two vertical sides are infinitesimal. Stokes theorem states that $\oint \left(\nabla \times \vec{E}\right) \cdot d\vec{a} = \oint \vec{E} \cdot d\vec{l}$. If the vertical paths are as short as we wish, E_t does not vary significantly over them and their integrals are zero. And the line integral of $\vec{E} \cdot d\vec{l}$ is $E_{t1}L–E_{t2}L$. By Stokes's Theorem, this line integral is equal to the integral of $\nabla \times \vec{E}$ over the surface enclosed by the path C [25–29].

By definition, the enclosed area is zero. So, $E_{t1}L–E_{t2}L = 0$, hence $E_{t1} = E_{t2}$. The tangential component of $\vec{E}$ is therefore continuous across the boundary. Applying this reasoning to the interface of a piece of food and the air in a microwave oven, as shown in **Figure 6(B)**, everything follows and the tangential component of $\vec{E}$ in the cooking chamber just above the surface of that matter is continuous with the tangential component of $\vec{E}$ just inside "the chicken."

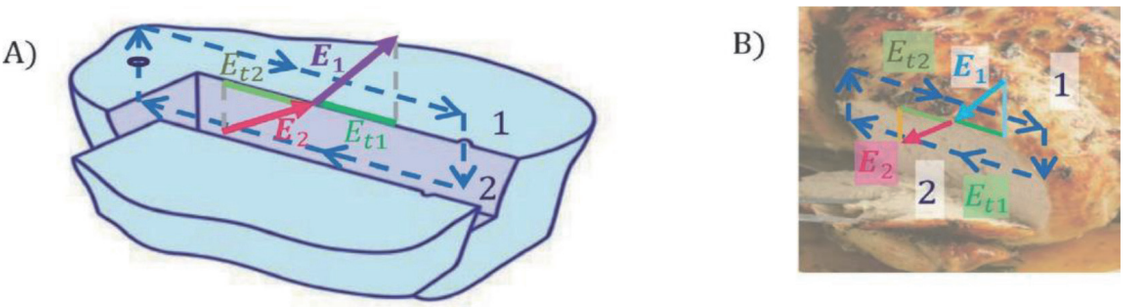

Figure 6.

Boundary condition on $\vec{E}$. (A) Closed path of integration crossing the interface between two different media 1 and 2. Whatever be the surface charge density σ_f, the tangential components of $\vec{E}$ on both sides of the interface are equal: $E_{t1} = E_{t2}$. The tangential components of $\vec{E}$ field are continuous no matter what medium 1 is and what medium 2 is. (B) The same analysis for a piece of chicken, or a cup of coffee, or melting cheese in a microwave oven follows: The tangential components of $\vec{E}$ are continuous. E_{t_2} contributes, at most, to some heating on the surface of the meal.

For the case of the metallic walls of the heating chamber and the walls of the waveguide, we have the case of a boundary between a dielectric (hot air) and a conductor, then $\vec{E} = 0$ in the conductor and $E_t = 0$ in both media. The magnetic part of the microwaves also obeys corresponding boundary conditions, namely: $B_{1n} = B_{2n}$ and $H_{1t} = H_{2t}$, and B_{2n} is quite capable of exciting magnetic dipoles inside the specimen, but food, beverages, water, and coffee do not possess magnetic moments, which are not magnetic. So, we do not treat here magnetic heating, even though it is a very active field of research [10, 11]. We concentrate on heating through electric dipoles inside the cooking chamber, as shown in **Figures 3, 5**, and **6**. Next, we describe more quantitatively the electromagnetics in the cooking chamber.

4. Microwave cooking chamber as a resonant cavity

Aforesaid, the empty cooking chamber in a microwave oven (MWO) is a closed rectangular space where, once microwaves are input, they bounce back and forth from metallic walls on the six sides and confine the electromagnetic waves in such space. This is an electromagnetic resonant cavity (ERC) in which electromagnetic waves (EMW) move in space and time periodically and, very importantly, forming standing wave patterns with nodes and anti-nodes. The cooking chamber is then electromagnetically a resonant cavity that imposes on the microwaves boundary conditions at the six walls. The $\vec{E}$ field, just outside and parallel to each wall, E_t, must be zero and the normal component of $\vec{B}$ must be continuous [25–29]. When food, water, coffee, cheese, or any other food are introduced in it, a dielectric medium with $\varepsilon \neq \varepsilon_0$ and air with $\approx \varepsilon_0$ are now the composite dielectric that fills the resonant cavity, as shown in **Figure 3**. Dielectrics do not perturb considerably the standing wave patterns that form the microwaves inside the MWO.

Let us be more quantitative, and take a standard microwave oven of dimensions a = 30 cm, b = 32 cm, and c = 38 cm as shown in **Figure 1(D)**. We will take the walls as perfect conductors as first approximation, boundary conditions on the six walls have to be fulfilled, and there will be multiple reflections at the metallic boundary surfaces. **Figure 7** shows how a sinusoidal electromagnetic field wave bounces back from a perfect conducting surface [25–29].

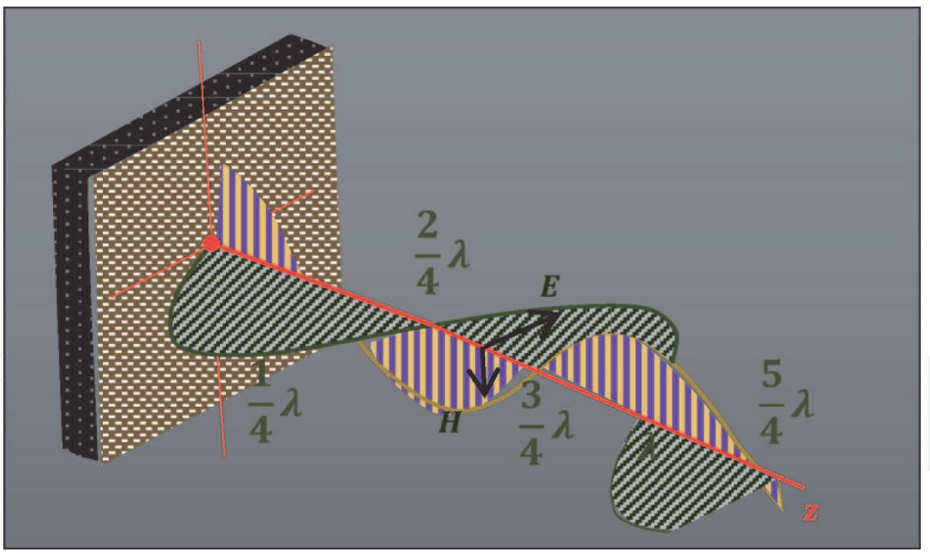

Figure 7.
The standing wave pattern resulting from the reflection of a microwave at the surface of a good conductor wall of the cooking chamber. The curvy lines show the standing waves of $\vec{E}$ and $\vec{H}$ at some particular time. The nodes $\vec{E}$ and of $\vec{H}$ are not coincident but are spaced λ/4 apart as shown. Modified from [25].

An arbitrary standing wave pattern in the resonant cavity can then be obtained as an appropriate superposition of these standing waves. Let us consider the closed region (cooking chamber) with walls of sides a, b, and c, and with the origin at one corner as shown in **Figure 3**. The cavity is filled with a linear dielectric, food (material described by μ_0 and ε). Both fields, $\vec{E}$ and $\vec{H}$, inside should obey Maxwell equations and each field component satisfies the wave equation; the solutions are stationary, confined, trapped microwaves. Applying separation of variables first to the time variable, it results in a solution of the form $e^{-i\omega t}$. Therefore, we have now, let us say, for

$$x\left(\vec{r},t\right) = \psi_0 = E_{0_x} X(x)Y(y)Z(z)e^{-i\omega t} \tag{1}$$

which, when substituted into the wave equation, leads to the Helmholtz equation $\nabla^2\psi_0 + k_0^2\psi_0 = 0$ where $k_0^2 = (\omega/\upsilon)^2$. This result is actually valid for any kind of coordinate system. Helmholtz equation is readily solved in rectangular coordinates by separation of variables. If we write, $\psi_0 = X(x)Y(y)Z(z)$ and proceed with the standard separations, we obtain [28, 29].

$$\begin{aligned}\Psi_0\left(\vec{r}\right) = &\left(C_1 \sin k_1 x + C_2 \cos k_1 x\right)\left(C_3 \sin k_2 y + C_4 \cos k_2 y\right)\\ &\times \left(C_5 \sin k_3 z + C_6 \cos k_3 z\right)\end{aligned} \tag{2}$$

where k_1, k_2, and k_3 are the wave numbers in the x, y, z dimensions and are related to the frequency ω of the microwave field by the dispersion relation $k_1^2 + k_2^2 + k_3^2 = k_0^2 = (\omega/\upsilon)^2$. Combining this $\psi_0\left(\vec{r}\right)$ with the temporal solution $T(t)$, we get any one of the components of the $\vec{E}$ and $\vec{H}$ field as

$$\begin{aligned}E_x = &\left(C_1 \sin k_1 x + C_2 \cos k_1 x\right)\left(C_3 \sin k_2 y + C_4 \cos k_2 y\right)\\ &\times \left(C_5 \sin k_3 z + C_6 \cos k_3 z\right)e^{-i\omega t}\end{aligned} \tag{3}$$

The boundary conditions that obey each $\vec{E}$ and $\vec{H}$ field component are going to make the difference of the fields through the fact that the constants, C_1, C_2, … , C_6, of

each component will take different values, including zero. The boundary condition $E_{1t} = E_{2t}$ at any metallic wall ($E_{metal} = 0$) makes for tangential components to be zero. Hence, E_x will be a tangential component and must therefore vanish at the faces $y = 0$ and b and $z = 0$ and c. We see that this requires that $C_4 = C_6 = 0$ and that $k_2 = n\pi/b$ and $k_3 = p\pi/c$ for $\sin(k_2 b) = 0$ and $\sin(k_3 c) = 0$, and where n and p are integers.

Then we have for E_x:

$$E_x = \left(C_1' \sin k_1 x + C_2' \cos k_1 x\right) \sin k_2 y \sin k_3 z e^{-i\omega t} \tag{4}$$

where $C_1' = C_1 C_3 C_5$ and $C_2' = C_2 C_3 C_5$. Repeating this whole procedure for E_y and its boundary conditions and for E_z and its boundary conditions we get

$$E_y = \sin k_1 x \left(C_3' \sin k_2 y + C_4' \cos k_2 y\right) \sin k_3 z e^{-i\omega t} \tag{5}$$

$$E_z = \sin k_1 x \sin k_2 y \left(C_5' \sin k_3 z + C_6' \cos k_3 z\right) e^{-i\omega t} \tag{6}$$

and $k_1 = m\pi/a$. Substituting the expressions of k_1, k_2, k_3 into the dispersion relation, we obtain all the possible frequencies of oscillation in this cooking chamber of a, b, c dimensions

$$\left(\frac{\omega}{\nu}\right)^2 = \left(k_1^2 + k_2^2 + k_3^2\right) = \pi^2 \left[\left(\frac{m}{a}\right)^2 + \left(\frac{n}{b}\right)^2 + \left(\frac{p}{c}\right)^2\right] \tag{7}$$

Notice that $k_1 = k_m$, $k_2 = k_n$, and $k_3 = k_p$. Each set of integers (n, m, p) define a mode of $\vec{E}$ field. From this relation aforesaid, we see that frequency ω takes only particular values determined by m/a, n/b, and p/c. There are many combinations of (n, m, p) called modes and then corresponding k values and "mode" frequencies ω_{nmp}. Each ω_{nmp} is a mode of vibration of the electric field and of the $\vec{H}$ field (that we obtain below).

It is important to note that if any two of the integers m, n, p are zero, then the other corresponding two k_1, k_2, k_3 are zero, and from the expressions for E_x, E_y, E_z we see then that all three components of $\vec{E}$ are zero. Hence, as a consequence all components of $\vec{H}$ become zero since $\vec{H} = \xi \vec{k} \times \vec{E}$ and no standing wave pattern is sustained in the cooking chamber. We define the vector wave number $\vec{k}$ with components $k_1 = k_n$, $k_2 = k_m$, and $k_3 = k_p$. The vector electric field must satisfy Maxwell's equations and, in particular, the first Maxwell equation (Gauss Law in differential form) with $\rho_f = 0$. We must have $\varepsilon \nabla \cdot \vec{E} = 0$. To apply divergence we construct $\partial Ex/\partial x$, $\partial Ey/\partial y$, $\partial Ez/\partial z$ with the field components above, we obtain

$$\begin{aligned} &-\left(k_1 C_2' + k_2 C_4' + k_3 C_6'\right) \sin k_1 \mathrm{x} \sin k_2 y \sin k_3 z \\ &+\left[\left(k_1 C_1' \cos \mathrm{k_1 x} \sin k_2 y \sin k_3 z\right) + \left(k_2 C_3' \sin k_1 \mathrm{x} \cos k_2 y \sin k_3 z\right)\right. \\ &\left.+\left(k_3 C_3' \sin \mathrm{k_1 x} \sin k_2 y \cos k_3 z\right)\right] = 0 \end{aligned} \tag{8}$$

The three terms on the left must sum up to zero. One way to have this zero is to ask for each term individually be zero, then we set $k_1 \mathrm{C'}_2 + k_2 \mathrm{C'}_4 + k_3 \mathrm{C'}_6 = 0$ *and also* $\mathrm{C'}_1 = \mathrm{C'}_3 = \mathrm{C'}_5 = 0$. The only surviving constants are C'_2, C'_4, and C'_6 and the resulting field components are now

$$E_x = \left(C_2' \cos \mathrm{k_1 x}\right) \sin k_2 y \sin k_3 z e^{-i\omega t} \tag{9}$$

$$E_y = \sin k_1 x \left(C_4' \cos \mathrm{k_2} y\right) \sin k_3 z e^{-i\omega t} \tag{10}$$

$$E_z = \sin k_1 x \sin k_2 y \left(C_6' \cos \mathrm{k}_3 z\right) e^{-i\omega t} \tag{11}$$

The amplitude of each of these waves is C_2', C_4', and C_6'. So, let us rename them as $C_2' = E_1$, $C_4' = E_2$, and $C_6' = E_3$, we find that the last conditions can be written as [28, 29].

$$k_1 E_1 + k_2 E_2 + k_3 E_3 = \vec{k} \cdot \vec{E} = 0 \tag{12}$$

The expressions for the field components finally become

$$E_x(x, y, z; t) = E_1 \cos k_1 \mathrm{x} \sin k_2 y \sin k_3 z e^{-i\omega t} \tag{13}$$

$$E_y(x, y, z; t) = E_2 \sin k_1 \mathrm{x} \cos k_2 y \sin k_3 z e^{-i\omega t} \tag{14}$$

$$E_z(x, y, z; t) = E_3 \sin k_1 \mathrm{x} \sin k_2 y \cos k_3 z e^{-i\omega t} \tag{15}$$

So that E_1, E_2, and E_3 are the amplitudes of the respective components.

We now show, in **Figure 8**, a 3D plot of the E_y component for the mode $n = 2$, $m = 4$, $p = 3$, and a 3D plot of the E_z component for the mode $n = 3$, $m = 5$, $p = 2$. It is immediately apparent that the number of maxima, minima, and nodes increases as the mode number (n, m, p) increases. Both plots show in the horizontal plane the projections of these maxima and minima. When thinking in the rectangular microwave cavity, this 2D plot represents the heating power at different spots at a z = constant plane (height in the microwave oven). This is just a very simplified picture of what the hot and cold spots are inside the 3D microwave chamber. The whole hot/cold distribution spots are the superpositions of many (n, m, p) electromagnetic standing wave patterns.

The color code used in **Figure 8(A)** and **(B)** represents maxima (red) and minima (blue) of the electric field of the microwaves. Since the energy delivered to

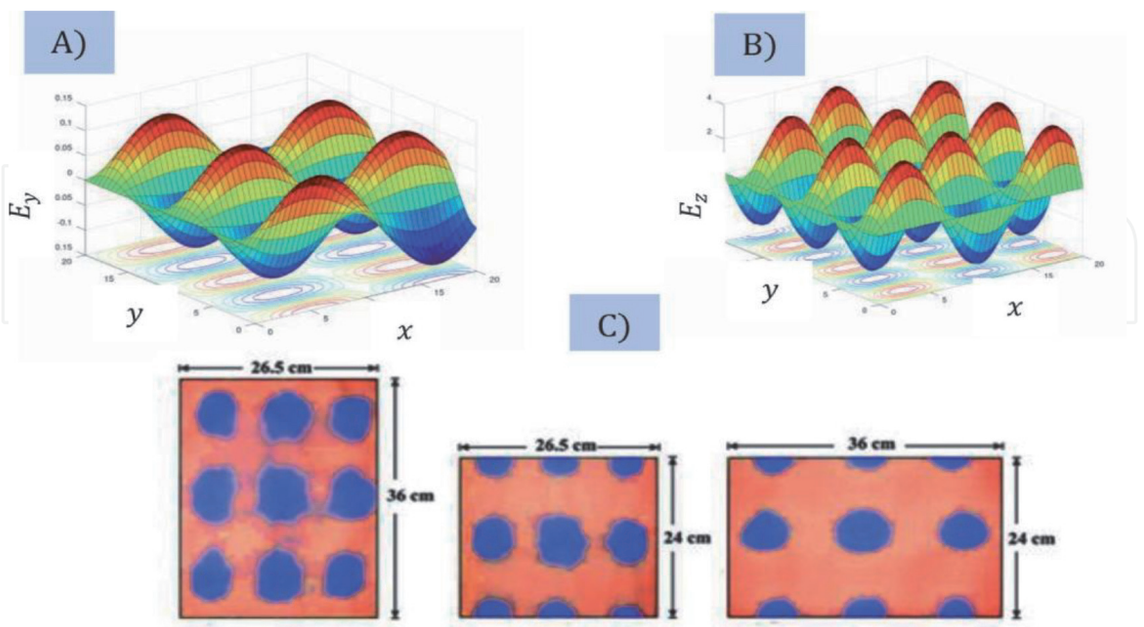

Figure 8.
Calculated and experimental electric field stationary wave patterns inside a rectangular cavity. (A) 3D plot of the E_y *stationary pattern for the mode* n = 2, m = 1, p = 3, *evaluated from Eq. (14) at an arbitrary* z *fixed value. (B) 3D plot of the* E_z *stationary pattern for the mode* n = 2, m = 1, p = 3, *evaluated from Eq. (15) at an arbitrary* z *fixed value. In both cases, the projection in the* x–y *plane of the maxima, minima, and nodes is shown. (C) The experimental determination of the hot/cold spots in a rectangular chamber,* a = 36 cm, b = 24 cm, *and* c = 26.5 cm. *Note the alternating pattern of hot/cold spots in the stationary pattern (adapted from [30]).*

the sample goes as the square of the electric field, then red and blue extrema become hot spots and the nodes become cold spots and are located between the red and blue spots. In the 2D projection, the regions between the blue and red zones are the cold spots. Experimental measurements on the standing wave patterns in microwave ovens have been reported and nicely agree with the theoretical calculations [30, 31]. In **Figure 8(C)**, we show one of those measurements carried out on three perpendicular planes, x–z, y–z, and x–y. The agreement between our calculations, planar 2D plots, and the experimental hot/cold spots in **Figure 8** is very satisfactory. The general pattern calculated and measured in the three planes consists of alternating maxima, minima, and nodes for each mode (n, m, p) as given by formulas (12)–(15).

The results in Eqs. (12)–(15) are very much like that one found for a plane wave [25–29]. Thus, for a given mode, a particular set (n, m, p), $\vec{E}_0$ must be perpendicular to the vector $\vec{k} = (m\pi/a)\hat{x} + (n\pi/b)\hat{y} + (p\pi/c)\hat{z}$.

For cylindrical cavities, stationary electromagnetic wave patterns are also obtained. Cylindrical cavities are very frequently used in research and in industrial applications as we showed above in **Figure 2(C)** for decomposition of waste plastics into H_2 and a set of fullerene solid compounds. Here, without any calculations, we show in **Figure 9** the electric field stationary wave pattern that we simulated from the cylindrical solutions for the TM_{010} mode. It is shown as a manner of contrast with the stationary pattern that results in rectangular geometry.

Calculating the magnetic field, we start from our knowledge of $\vec{E}$ and of the vector wave number $\vec{k}$. From the third Maxwell equation, we have $\nabla \times \vec{E} = -\mu\left(\frac{\partial \vec{H}}{\partial t}\right) = i\omega\mu\vec{H}$. For example, using the expressions for E_x, E_y, E_z just found above, we have

$$i\omega\mu H_x = \frac{\partial E_z}{\partial y} - \frac{\partial E_y}{\partial z} = (k_2E_3 - k_3E_2)\sin k_1 x \cos k_2 y \cos k_3 z e^{-i\omega t}. \tag{16}$$

Since k_2E_3–k_3E_2 is the x component of $\vec{k} \times \overrightarrow{E_0}$, it is desirable to define a vector $\overrightarrow{H_0}$ by $\overrightarrow{H_0} = \frac{1}{\omega\mu}\vec{k} \times \overrightarrow{E_0}$ for, if we let its rectangular components be H_1, H_2, and H_3, then we can write H_x as

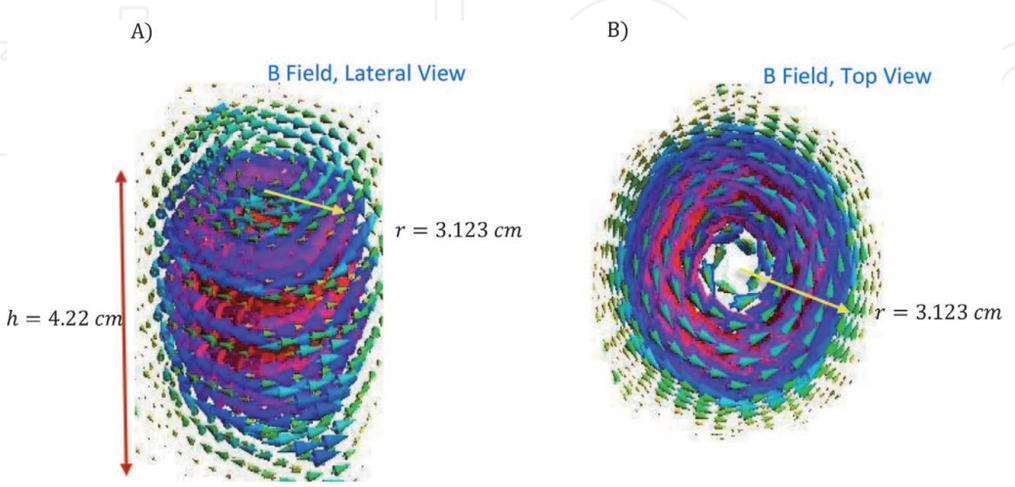

Figure 9.
Simulation of the stationary pattern of the electric field inside a cylindrical resonant cavity, TM_{010} mode. (A) The electric field is concentric with minima close to r = 0, *and* $\vec{E}$ = 0 *exactly at* r = 0. *The field is tangent to the metallic wall and very small at* R = r. *(B) A top view of the same electric field stationary pattern [19]. This stationary field configuration is established in cylindrical cavities, TM_{010} mode, used for research at low microwave powers to excite magnetic specimens.*

$$H_x = -iH_1 \sin(k_1 x) \cos(k_2 y) \cos(k_3 z) e^{-i\omega t} \tag{17}$$

Similarly, we find the other two components of $\vec{H}$ to be

$$H_y = -iH_2 \cos(k_1 x) \sin(k_2 y) \cos(k_3 z) e^{-i\omega t} \tag{18}$$

and

$$H_z = -iH_3 \cos(k_1 x) \cos(k_2 y) \sin(k_3 z) e^{-i\omega t} \tag{19}$$

We see that $H_x = 0$ at $x = 0$ and $x = a$, that is, at the walls for which it is a normal component; similarly, H_y and H_z vanish at $y = 0$ and b and $z = 0$ and c, respectively. Thus, the boundary conditions on $\vec{H}$ have been automatically satisfied once $\vec{E}$ was made to satisfy its own boundary conditions. Furthermore, it is easily verified that the two remaining Maxwell equations that we have not yet used are satisfied, that is, $\nabla \cdot \vec{H} = 0$ and $\nabla \times \vec{E} = -\left(\partial \vec{B}/\partial t\right)$ One needs to use $\vec{k} \cdot \vec{H_0} = 0,$ as well as $\boldsymbol{H}_x E_z$ and the relation dispersion in its form $\vec{k} \cdot \vec{k} = k_0^2 = \frac{\omega^2}{v^2} = \omega^2 \mu \varepsilon$. Each component of $\vec{E}$ varies as $e^{-i\omega t}$, while the components of $\vec{H}$ are proportional to $-ie^{-i\omega t} = e^{-i\left[\omega t + \left(\frac{1}{2}\right)\pi\right]}$. Thus, the electric and magnetic fields are not in phase in these standing waves but instead $\vec{H}$ leads $\vec{E}$ by 90° as shown in **Figure 7**. A given $\vec{k}$ corresponds to a given mode, that is, a given set of integers m, n, p in k aforesaid. Now $\vec{k} \cdot \vec{E}$ tell us that the vector E_0 must be chosen to be perpendicular to $\vec{k}$. However, there are two independent mutually perpendicular directions along which $\vec{E_0}$ can be chosen and still be perpendicular to a $\vec{k}$.

Thus, for each possible value of $\vec{k}$, there are two possible independent directions of polarization of $\vec{E_0}$, so that there are two distinct modes for each allowed frequency given by ω_{nmp}. This property is known as degeneracy and is a fundamental and important feature of electromagnetic standing waves. If a, b, c are all different, then the various frequencies given by ω_{nmp} will generally be different. However, if there are simple relations among the dimensions, it is possible that different choices of the integers will give the same frequency so that we will also have degeneracy, but arising in a different manner. As an extreme example, consider a cube for which $a = b = c$, so that ω_{nmp} reduces to $\left(\frac{\omega}{v}\right)^2 = \left(\frac{\pi}{a}\right)^2 (m^2 + n^2 + p^2)$. Thus, all combinations of integers that have the same value of $m^2 + n^2 + p^2$ will have the same frequency and the modes will be degenerate.

5. The Poynting vector of the microwave fields inside the cooking chamber

Remembering that $\vec{S}(r,t) = \vec{E}(r,t) \times \vec{H}(r,t)$, taking the expressions of $\vec{E}$ and $\vec{H}$ Inside the cooking chamber, then we obtain $\vec{S}(r,t) = \ |E||H|\hat{k} = \xi \cdot \upsilon \cdot (\varepsilon/2) E^2 \hat{k} = \xi \cdot vu\hat{k}$ [25–29]. This result is the general one obtained in any electrodynamic circumstance, of course, and microwave ovens fulfill it. And the average Poynting vector is $Sav = Power/Area = Energy/Area \cdot time$. What these expressions tell us is that microwave energy and microwave power inside the cooking chamber are

traveling-moving, yes energy, and power, between the six walls in stationary wave patterns and in accord with the propagation vector $\vec{k}$ and carrying perpendicular to it the $\vec{E}$ and $\vec{H}$ fields. The microwave power deposited on a surface area of 1 mm^2 is then $Pav = Sav.A$. Since $\vec{E}$ and $\vec{H}$ inside the microwave oven have nodes and anti-nodes, then $\overrightarrow{S}(r,t)$ and consequently microwave power, $P(r,t)$ have nodes and anti-nodes at some positions along x, y, and z, and the heating is not uniform due to this standing wave feature of the microwave fields inside the cavity. Experimental results on the standing wave patterns have been reported and nicely agree with the theoretical calculations [30, 31]. Theoretically and experimentally standing microwave patterns are obtained. The reason of the rotating plate is to move in circular fashion the food to be heated and reach a more uniform microwave bathing on the food. Most of the time it is accomplished, but not always, as pizza fans report.

Now that we have a detailed treatment of the electromagnetic fields inside the cooking chamber, we want to develop some expressions for the $\vec{E}$ and $\vec{H}$ fields traveling on the waveguide from the magnetron toward the resonant cavity.

6. The waveguide in microwave heating systems, TE and TM modes

In research and technologically bound situations, the resonant cavities we saw above are feed with microwaves by means of waveguides connecting the source to the microwave cavity, see **Figures 2** and **4**. We can think of a waveguide as constructed from a cavity by taking the $\pm z$ walls to infinity; then, the trapped stationary waves in the cavity can now travel indefinitely toward $\pm$ infinity as plane waves. As soon as we start taking the $\pm z$ walls to infinity, we start liberating boundary conditions and in that dimension we are allowing free traveling waves. The remaining walls at $x = 0$, a, and $y = 0$, b continue limiting our bouncing waves along these dimensions. We will continue taking the bounding surfaces as perfect conductors. A question to ask at this point is; Is it possible to transfer electromagnetic energy along a *waveguide*, that is, a tube with open ends? From everyday experience, we already know that this is possible from the simple fact that we can see through long straight pipes. So, the answer is yes, but: How is this carried out? Solutions to the wave equations have the answer, but first we review quickly boundary conditions on perfect conductors.

7. Boundary conditions at the surface of a perfect conductor

We recall that a *perfect conductor* is one for which $\sigma \to \infty$, more precisely, one for which the ratio $Q = \varepsilon\omega/\sigma \to 0$. $Q \leq (1/50) \ll 1$ for common metals even at very high frequencies so that $Q = 0$ should be a good first approximation for metallic boundaries. Plane waves traveling freely along the z direction take the form $E(x,y)\ \exp\ [i(\omega t - kz)]$, where the $E(x,y)$ part has to be found but we already know that fulfills boundary conditions at the metallic walls. We remember that $\delta = (2/\mu\sigma\omega)^{1/2}$ for a good conductor so that $\delta \to 0$ as $\sigma \to \infty$. Therefore, the electric field is zero at any point in a perfect conductor since the skin depth is zero. Since the tangential components of $\vec{E}$ are always continuous, we see that $\vec{E}_{tang} = 0$ just outside of the surface. In other words, $\vec{E}$ has no tangential component at the surface of a perfect conductor so that $\vec{E}$ must be normal to the surface [25–29]. $\overrightarrow{B}$ inside the

conductor is $\vec{B} = (k/\omega)\vec{k} \times \vec{E_\tau}$ so that $\vec{B}$ will also be transverse. Consequently, the transverse component of $\vec{B}$ inside will also vanish as $\sigma \to \infty$. Since $\vec{B}$ has no normal component, the boundary condition $B_{1n} = B_{2n}$ implies that $\vec{B}_{norm} = 0$ just outside the conductor. Thus, at the surface of a perfect conductor and outside of it, $\vec{B}$ has no normal component; that is, it must be tangential to the surface. We see that *all* of the field vectors will be zero inside a perfect conductor. This simplifies greatly the general boundary conditions. To repeat: At the surface of a perfect conductor, $\vec{E}$ is normal to the surface and $\vec{B}$ is tangential to the surface. To put it another way, $\vec{E}$ has no tangential component while $\vec{B}$ has no normal component.

8. Propagation characteristics of waveguides

Figure 10 shows a waveguide that extends indefinitely in the z direction and of arbitrary and constant cross section in the xy plane. We take the boundary walls as perfect conductors and the interior of the cavity is filled with a linear nonconducting medium described by μ_0 and ε. If ψ is any component of $\vec{E}$ or $\vec{B}$, we know that it satisfies the scalar wave equation $\nabla^2\psi - \frac{1}{v^2}\frac{\partial^2\psi}{\partial t^2} = 0$ where $v^2 = 1/\mu\varepsilon$ and v would be the speed of a plane wave in the medium. Again, by separation of variables we easily find $\psi(x,y,z,t) = \psi_0(x,y)e^{i(k_g z - \omega t)}$.

We note that this is *not* a plane wave since the amplitude ψ_0 is not a constant but depends on x and y, the cross section [28, 29]. The quantity k_g is the *guide propagation constant, or simply the k_z constant of separation of the Z(z) component* of the whole solution and can be written as $k_g = 2\pi/\lambda_g$ here λ_g is the guide wavelength, that is, the spatial period along the guide, the z axis.

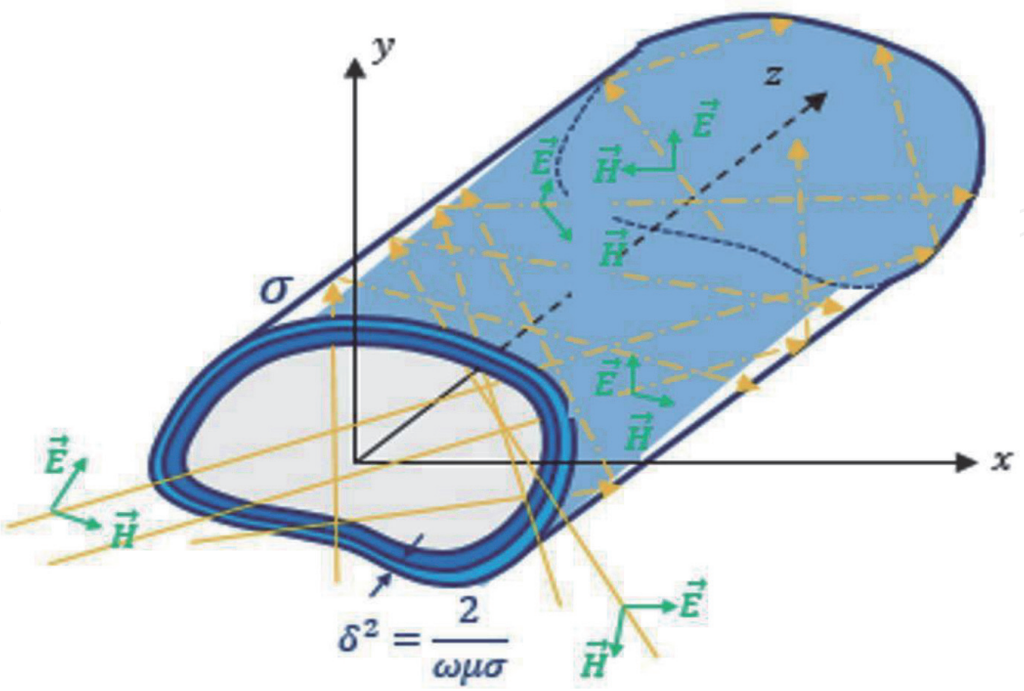

Figure 10.
A waveguide made of a perfect conductor with arbitrary and constant cross section. A set of propagation vectors k_1, k_2, k_3, etc., are shown to impinge on different points on the metallic walls and reflect back following Snell law. Transmission is not depicted since perfect conducting walls are considered, and hence, the skin depth tends to zero, which implies zero transmission.

Continuing with the separation of variables now for the x and y variables, we obtain again a Helmholtz equation in 2D $\frac{\partial^2\psi_0}{\partial x^2}+\frac{\partial^2\psi_0}{\partial y^2}+k_c^2\psi_0=0$, where $k_c^2=k_0^2-k_g^2$ and $k_0=\frac{\omega}{\upsilon}=\frac{2\pi}{\lambda_0}$. Writing $k_c=\frac{2\pi}{\lambda_c}$ we obtain a wavelength relation $\frac{1}{\lambda_c^2}=\frac{1}{\lambda_0^2}-\frac{1}{\lambda_g^2}$. Therefore, we have found for a waveguide that we will get wave propagation *only* if $k_0>k_c$, or $\lambda_0<\lambda_c$. For this reason, λ_c is called the *cutoff wavelength*. It is very common to state this result in terms of a cutoff frequency ωc defined by $k_c=\frac{\omega_c}{\upsilon}$ so that kg^2 can also be written as $k_g^2=\frac{1}{\upsilon^2}\left(\omega^2-\omega_c^2\right)$. Then, wave propagation is possible only if $\omega>\omega^2$, that is, if the applied frequency is greater than the cutoff frequency.

9. Rectangular guide

This guide has a rectangular cross section of sides a and b, which we take to be located in the xy plane. It is relevant to mention that for either type of mode, TE or TM, we have to solve an Helmholtz equation and apply boundary conditions as aforesaid. We continue using separation of variables and write $\psi_0(x,y)=X(x)Y(y)$; then, the same arguments as used in resonant cavity section above lead us to the separated equations

$$\frac{1}{X}\frac{\partial^2X}{\partial x^2}=-\frac{1}{Y}\frac{\partial^2Y}{\partial y^2}-k_c^2=\text{const.}=-k_1^2 \tag{20}$$

so that, $(d^2X/d\,x^2)+k_1^2X=0$ and $(d^2Y/d\,y^2)+k_2^2Y=0$ the separation constants have been selected with minus sign since the solutions should be periodic. Hence, $k_1^2+k_2^2=k_c^2$ is the dispersion relation in terms of the constants of separation for this 2D differential equation. Solving these in terms of sine and cosine functions, we find that $\psi_0(x,y)=(C_1\sin k_1x+C_2\cos k_1x)(C_3\sin k_2y+C_4\cos k_2y)$, where the C's are constants of integration. This expression for ψ_0 contains a total of four constants.

Let us calculate for TE *modes*. Here, we set $\mathcal{E}_z=0$ and write

$$\mathcal{H}_z=(C_1\sin k_1x+C_2\cos k_1x)(C_3\sin k_2y+C_4\cos k_2y) \tag{21}$$

With $\mathcal{E}_z=0$, and with $\nabla\times\vec{E}=-\partial\vec{B}/\partial\text{t}$, we find that when we substitute $\mathcal{H}_z$ into E_x and E_y coming from $\nabla\times\vec{E}$ and after some algebra [28].

$$\mathcal{E}_x=\frac{i\omega\mu k_2}{k_c^2}(C_1\sin k_1x+C_2\cos k_1x)(C_3\sin k_2y-C_4\cos k_2y) \tag{22}$$

$$\mathcal{E}_y=\frac{i\omega\mu k_1}{k_c^2}(C_1\cos k_1x-C_2\sin k_1x)(C_3\sin k_2y+C_4\cos k_2y) \tag{23}$$

From the boundary conditions $\mathcal{E}_x(y=0)=0$ and $\mathcal{E}_x(y=b)=0$ and similarly, from the boundary conditions that $\mathcal{E}_y(\text{x})=0$ must satisfy at $x=0$ and $x=a$, then evaluating first for the zero values of x and y, we get

$$\mathcal{E}_x(x,0)=0=\frac{i\omega\mu k_2C_3}{k_c^2}(C_1\sin k_1x+C_2\cos k_1x) \tag{24}$$

$$\mathcal{E}_y(0,y)=0=-\frac{i\omega\mu k_1C_1}{k_c^2}(C_3\sin k_2y+C_4\cos k_2y) \tag{25}$$

Notice that we have here established a 2D homogeneous Sturm-Liuville problem and we expect to obtain as solutions eigenvalues and eigenfunctions. From the aforesaid boundary conditions, we must have $C_1 = 0$ and $C_3 = 0$. Therefore, at this stage, $\mathcal{E}_x$, $\mathcal{E}_y$, $\mathcal{H}_z$ have simplified to

$$\mathcal{H}_z = C_2C_4 \cos k_1x \cos k_2y \tag{26}$$

$$\mathcal{E}_x = -\frac{i\omega\mu k_2C_3}{k_c^2} C_2C_4 \cos k_1x \sin k_2y \tag{27}$$

$$\mathcal{E}_y = \frac{i\omega\mu k_1C_1}{k_c^2} C_2C_4 \sin k_1x \cos k_2y \tag{28}$$

We still have boundary conditions to satisfy at the two remaining faces. We see that the requirement $\mathcal{E}_x(x,b) = 0$ leads to $\sin k_2b = 0$ so that $k_2b = n\pi$ where n is an integer. Similarly, $\mathcal{E}_y(a,y) = 0$ gives the condition that $k_1a = m\pi$ with m an integer. Thus, we have found the eigenvalues $k_1 = \frac{m\pi}{a}$ and $k_2 = \frac{n\pi}{b}$, these are the eigenvalues of the solution. So that $k_1^2 + k_2^2 = k_c^2$ shows that the allowed values of ${k_c}^2$ are $k_{c\,mn}^2 = k_{c\,mn}^2\pi^2\left[\left(\frac{m}{a}\right)^2 + \left(\frac{n}{b}\right)^2\right]$. The cutoff wavelengths and frequencies can now be found by using ${k_c}^2$ above into our ${\lambda_c}^2$ and ${\omega_c}^2$ equations. The corresponding guide propagation constants are

$$k_g^2 = \left(\frac{2\pi}{\lambda_g}\right)^2 = k_0^2 - \pi^2\left[\left(\frac{m}{a}\right)^2 + \left(\frac{n}{b}\right)^2\right] \tag{29}$$

The only quantity left undetermined is the arbitrary amplitude C_2C_4 of $\mathcal{H}_z$. If we set $C_2C_4 = H_0$, then we find that the amplitudes of a general TE mode in a rectangular guide are as follows:

$\mathcal{E}_x = -\frac{i\omega\mu}{k_c^2}\left(\frac{n\pi}{b}\right)H_0 \cos\left(\frac{m\pi x}{a}\right)\sin\left(\frac{n\pi y}{b}\right)$	$\mathcal{H}_x = -\frac{ik_g}{k_c^2}\left(\frac{m\pi}{a}\right)H_0 \sin\left(\frac{m\pi x}{a}\right)\cos\left(\frac{n\pi y}{b}\right)$
$\mathcal{E}_y = \frac{i\omega\mu}{k_c^2}\left(\frac{m\pi}{a}\right)H_0 \sin\left(\frac{m\pi x}{a}\right)\cos\left(\frac{n\pi y}{b}\right)$	$\mathcal{H}_y = -\frac{ik_g}{k_c^2}\left(\frac{n\pi}{b}\right)H_0 \cos\left(\frac{m\pi x}{a}\right)\sin\left(\frac{n\pi y}{b}\right)$
$\mathcal{E}_z = 0$	$\mathcal{H}_z = H_0 \cos\left(\frac{m\pi x}{a}\right)\sin\left(\frac{n\pi y}{b}\right)$

where k_c and k_g are as above. Multiplying each of these amplitude factors by the wave propagation term we get, for example, for the E_x field

$$E_x = -\frac{i\omega\mu}{k_c^2}\left(\frac{n\pi}{b}\right)H_0 \cos\left(\frac{m\pi x}{a}\right)\sin\left(\frac{n\pi y}{b}\right)e^{i\left(k_gz-\omega t\right)} \tag{30}$$

Since $-i = e^{-i(1/2)\pi}$, the exponential factor can be written $\exp i\left[k_gz - \left(\omega t + \frac{1}{2}\pi\right)\right]$, which shows that E_x leads H_z in time by 90°. Similarly, H_x and H_y lead H_z by 90° while E_y lag H_z by this same amount.

We now particularize to the simplest case which is also the most used. The TE_{10} *mode*, we set m = 1 and $n = 0$ and we particularize the above equations for these particular values of m and n, we show now without calculations that:

$$k_g = \left[\left(\frac{\omega}{v}\right)^2 - \left(\frac{\pi}{a}\right)^2\right]^{1/2}.$$

The field amplitudes are

$$\mathcal{E}_y = i\omega\mu\left(\frac{a}{\pi}\right)H_0 \sin\left(\frac{\pi x}{a}\right) \tag{31}$$

$$\mathcal{H}_x = -ik_g\left(\frac{a}{\pi}\right)H_0 \sin\left(\frac{\pi x}{a}\right) \tag{32}$$

$$\mathcal{H}_z = H_0 \cos\left(\frac{\pi x}{a}\right) \tag{33}$$

While $\mathcal{E}_x = \mathcal{E}_z = 0$ and $\mathcal{H}_y = 0$. Inserting these amplitudes into the complete $\vec{E}$ and $\vec{H}$ field expressions above and taking the real parts of the resulting expressions, we find the only nonzero field components to be

$$E_y = -H_0\omega\mu\left(\frac{a}{\pi}\right) \sin\left(\frac{\pi x}{a}\right) \sin\left(k_g z - \omega t\right) \tag{34}$$

$$H_x = H_0 k_g\left(\frac{a}{\pi}\right) \sin\left(\frac{\pi x}{a}\right) \sin\left(k_g z - \omega t\right) \tag{35}$$

$$H_z = H_0 \cos\left(\frac{\pi x}{a}\right) \cos\left(k_g z - \omega t\right) \tag{36}$$

We see that the values of the E_y are independent of y; hence, the electric field lines are straight lines with constant magnitude at a given value of x but with a magnitude that does vary with x and is a maximum at the center where $x = (a/2)$. The lines of H_x are straight with their maximum value at the center as well. The value of H_z, on the other hand, is zero in the center as has opposite signs on the two sides of the center.

TM *modes*. In this case, we set $\mathcal{H}_z = 0$ and set $\mathcal{E}_z$ equal to the expression for ψ_0 given above; hence, $\nabla \times \vec{E} = -\partial\vec{B}/\partial t$ is again applicable. This case is actually simpler because $\mathcal{E}_z$ can be a tangential component and must vanish for $x = 0$ and a and $y =$ and b. We have again an homogeneous Sturm-Liouville problem and expect eigenvalues and eigenfunctions. Proceeding in the same manner as before, we see that we must now have $C_2 = C_4 = 0$, while k_1, k_2, and k_c are given, again as above. Thus, the TE and TM modes of a rectangular waveguide have the same set of cutoff wavelengths, the same eigenfrequencies, and cutoff frequencies; the field configurations can be expected to be different however. Setting $C_1C_3 = E_0$, we find that (21) gives the starting point for the TM calculation to be $\mathcal{E}_z = E_0 \sin\left(\frac{m\pi x}{a}\right) \sin\left(\frac{n\pi y}{b}\right)$. We now use this $\mathcal{E}_z$ to calculate the rest of the field amplitudes following the above procedure. We note that $m = n = 0$ makes $\mathcal{E}_z$ and then all the other field components, zero; thus, there is no TM_{00} mode. Furthermore, if $m = 0$ or $n = 0$, $\mathcal{E}_z = 0$ and all of the fields are zero. Thus, it is not possible to have a TM_{m0} or TM_{0n} mode, in contrast to the TE case.

We have now calculated in detail the electric and magnetic fields that propagate in rectangular waveguides as the ones shown in **Figures 1(B), 2(A)**, and **3(C)**. The field patterns are stationary wave patterns in the x–y direction and traveling waves along the z direction as given by Eqs. (30)–(36).

Let us proceed now to the last of the physical components of a microwave heater, the very source of 1000 Watts microwaves.

10. Radiation of accelerated point charges in klystrons and magnetrons

Klystrons and magnetrons produce microwaves that carry power; typically, klystrons are used when little power is needed, from 1 watt to milliwatts and even

microwatts. Magnetrons are used in higher-power applications, 1000 Watts, or more. Clearly, magnetrons are better suited for microwave heating. Both rely on electrons being accelerated (these electrons are labeled e_m) and made move in periodic trajectories inside cylindrical chambers. Both devices are shown in **Figure 11**. Notice the motion of electrons in them. Straight trajectories in klystrons, $w(t)$, **Figure 11(A)**, and curved trajectories, $\zeta(t)$, in magnetrons, see **Figure 11(B)**. To expose relevant physics of accelerated electrons, em, produced in klystrons and Magnetrons is to describe the $\vec{E}_{rad}$ and $\vec{B}_{rad}$ microwave radiation fields produced inside their structures and from these, the Poynting vector, $\vec{S}\left(\vec{r},t\right) = \vec{E}_{rad} \times \vec{H}_{rad}$ that describes flux of such energy through space.

A microwave power, $P_{rad} = \left|\vec{S}\right| \cdot Area$, comes with this traveling energy. For klystrons, the accelerated electrons travel along straight lines, inside vacuum tubes, back and forth, due to voltage differences, $\Delta V_{12} \geq 860$ Volts, applied at the ends of the cylindrical tube (chamber), see **Figure 11(A)**. So acceleration is linear and is $\vec{a}(z,t) = {}^{d\vec{v}(z)}/_{dt} = \frac{d^2\vec{w}(z,t)}{dt^2} = \ddot{\vec{w}}(z,t)$, in which $\vec{a} = \ddot{\vec{w}}$ is parallel to $\vec{v}$ and parallel to the tube axis, $\vec{z}$, see **Figure 11(A)**, and the acting force producing such acceleration is $\vec{F} = e\vec{E} = e(-\nabla V_{12})$. For magnetrons, the trajectories of the accelerated electrons are wavy circular with average radius $a \leq r \leq b$, as shown in **Figure 11(B)** and **(C)**. The wavy $\vec{\zeta}\left(\vec{r},t\right)$ trajectories of the accelerated electrons in magnetrons are the effect of a combined magnetic force $\vec{F}_{mag} = q\dot{\vec{\zeta}}\,(t)xB\hat{e}_z$ and the total electric force between these electrons and the charges located in pairs along the b radius, $\sigma \pm$ and $-Q$ at the cathode. What we have now is, charged particles, e_m, moving along trajectories, $\vec{w}(z,t)$, in klystrons, and $\vec{\zeta}(z,t)$, in magnetrons, both have velocities $\dot{\vec{w}}\,(z,t)$, $\dot{\vec{\zeta}}\,(z,t)$, and accelerations, $\ddot{\vec{w}}(z,t)$, $\ddot{\vec{\zeta}}\,(z,t)$. Charged particles in motion produce electric potentials and electromagnetic fields just as static charges do,

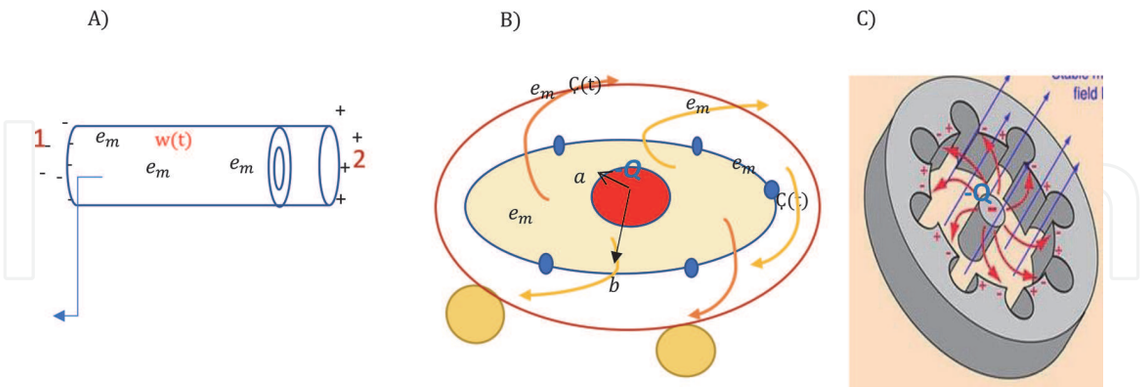

Figure 11.
Microwave sources, reflex klystron, and magnetron. (A) The basics of a klystron that produces accelerated electrons through an alternating electric potential difference $\Delta V_{12}(\omega t)$*, these* e_m *travel the distance* d*; then, the acceleration is reversed,* e_m *travel to the left now, and this repeats thousands of times at a GHz frequency. (B) In a magnetron hot electrons ejected from a central cathode, travel in circular-wavy trajectories inside a cylinder due to the Lorentz force* $\vec{F} = e\left(\vec{E} + \vec{v}(t)xB\hat{e}_z\right)$*, where* $\vec{v}(t) = \partial\vec{\zeta}\left(\vec{r},t\right)/\partial t = \dot{\vec{\zeta}}\,\left(\vec{r},t\right)$ *is the velocity of the* e_m *electrons,* $\vec{E}$ *is the total electric field due to the perimetral charges (+, −), (+, −), (+, −), and the central* −Q *charge.* $\vec{B}$ *is a constant magnetic field (from a magnet) applied along the* $\hat{e}_z$ *axis. These two forces combined produce the curved-wave trajectory* $\vec{\zeta}\left(\vec{r},t\right)$*. (C) A complete diagram of the magnetron structure with the constant magnetic field* $B\hat{e}_z$*, the charge distribution (proper of magnetrons) that produces a total* $\vec{E}$ *field and the curved electron trajectories* $\vec{\zeta}\left(\vec{r},t\right)$*.*

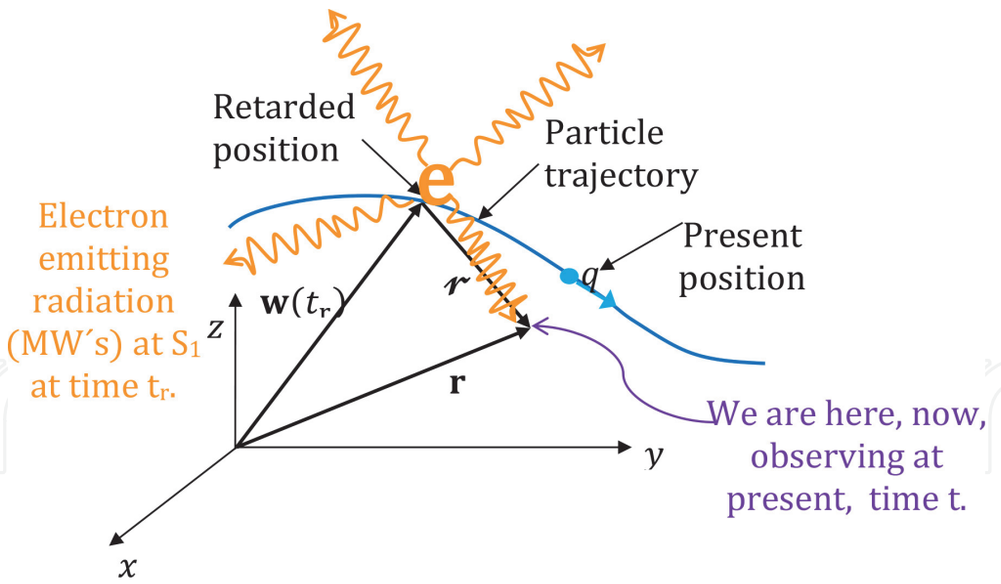

Figure 12.
A moving charged particle following a trajectory w(tr). $|\vec{r}\text{-}\vec{w}(t_r)|$ *is the distance the "radiated field" from the moving electron must travel, and* $(t - t_r)$ *is the time it takes to make the trip, we shall call* $\vec{w}(t_r)$ *the* ***retarded position*** *of the charge,* $\vec{\boldsymbol{r}}$ *is the vector distance from the retarded position to the point the radiated electromagnetic wave arrived "to us" (now, at our time* t_2*), which is at* $\vec{r}$*, clearly* $\vec{\boldsymbol{r}} = \vec{r}\text{-}\vec{w}\ (t_r)$.

except that here we have to calculate retarded potentials and retarded fields. For single charged particles, the resulting potentials are the well-known Lienard-Wiechert potentials [26–29, 32]. We present them here now. We take an accelerated electron moving in a general trajectory given by $\vec{\varsigma}\left(\vec{r},t\right)$, or $w(r,t) \equiv$ position of q at time t. Now, $V\left(\vec{r},t\right) = \frac{1}{4\pi\epsilon_0}\int\frac{\rho\left(\vec{r}',t_r\right)}{\boldsymbol{r}}d\tau'$ gives the electric potential at r at time t (**Figure 12**) [2, 26–29].

The retarded integration is not trivial, and the retardation in the $q/\boldsymbol{r}$ term in the potential aforesaid throws in a factor $\frac{q}{1-\vec{\boldsymbol{r}}\cdot\vec{\mathrm{v}}/c}$, where $\vec{\mathrm{v}}$ is the velocity of the charge at the retarded time, and $\vec{\boldsymbol{r}}$ is the vector from the retarded position to the point $\vec{r}$ where we are standing and measuring [24, 26–29, 32]. Then, $\int\rho\left(\vec{r}',t_r\right)d\tau' = \frac{q}{1-\vec{\boldsymbol{r}}\cdot\vec{\mathrm{v}}/c}$. It follows, then, that $V\left(\vec{r},t\right) = \frac{1}{4\pi\epsilon_0}\frac{qc}{\left(\boldsymbol{r}c-\vec{\boldsymbol{r}}\cdot\vec{v}\right)}$. Meanwhile, since the current density of a rigid object is $\vec{J} = \rho\vec{v}$, we also have $\vec{A}\left(\vec{r},t\right) = \frac{\mu_0}{4\pi}\int\frac{\rho\left(\vec{r}',t_r\right)\vec{\mathrm{v}}(t_r)}{\boldsymbol{r}}d\tau' = \frac{\mu_0}{4\pi}\frac{\vec{\mathrm{v}}}{\boldsymbol{r}}\int\rho\left(\vec{r}',t_r\right)d\tau'$.

Or $\vec{A}\left(\vec{r},t\right) = \frac{\mu_0}{4\pi}\frac{qc\vec{\mathrm{v}}}{\boldsymbol{r}c-\vec{\boldsymbol{r}}\cdot\vec{v}} = \frac{\vec{\mathrm{v}}}{c^2}V\left(\vec{r},t\right)$. These are the famous Lienard-Wiechert potentials for a moving point charge. By using $\vec{E} = -\nabla\mathrm{V} - \partial\vec{A}/\partial t$ and $\vec{B} = \nabla\times\vec{A}$, the corresponding fields are evaluated. It seems to us that only two authors, Jefimenko and Griffiths, give detailed derivation of these fields. The differential operations should be carried out with great care as these authors do, and we refer to those calculations and just take their results here:

$$\vec{E}\left(\vec{r},t\right) = \frac{q}{4\pi\epsilon_0}\frac{\boldsymbol{r}}{\left(\vec{\boldsymbol{r}}\cdot\vec{u}\right)^3}\left[\left(c^2-v^3\right)\vec{u} + \vec{\boldsymbol{r}}\times\left(\vec{u}\times\vec{a}\right)\right] = \vec{\mathrm{E}}_{\mathrm{vel}} + \vec{\mathrm{E}}_{\mathrm{accl}} \qquad (37)$$

where $\vec{u} = c\hat{\vec{\boldsymbol{r}}} - \vec{v}$, and, very importantly, $\vec{\mathrm{E}}_{\mathrm{vel}}\ \alpha\ 1/\boldsymbol{r}^2$ and $\vec{\mathrm{E}}_{\mathrm{accel}}\ \alpha\ \boldsymbol{r}$. And the magnetic field is

$$\vec{B}\left(\vec{r},t\right)=\frac{1}{c}\vec{\boldsymbol{r}}\times\vec{E}\left(\vec{r},t\right) \tag{38}$$

$\vec{B}$ follows the same time dependence as $\vec{E}$. The first term in $\vec{E}$ $(\vec{r},t)$ is called the **velocity field**, and the triple cross-product is called the **acceleration field**. With these potentials and Jefimenko fields, we are now in the position to describe more quantitatively the radiation produced in klystrons and magnetrons. Hence, the accelerated electrons, e_m, inside these devices produce V and $\vec{A}$ potentials and $\vec{E}$ and $\vec{B}$ fields. In klystrons, the radiation fields are, as they are, captured by the mouth of a waveguide and send to a resonant cavity in which they produce standing patterns of stationary microwaves for their use.

Finally, in magnetrons, the perimetral charges, $\sigma\pm$ experience Lorentz forces due to these Jefimenko fields, $\vec{F}=q^{\mp}\left(\vec{E}_J+\dot{\vec{\varsigma}}(t)x\vec{B}_J\right)$; hence, these charges move inside the conducting core behind radius b and around the cylindrical cavities, see **Figure 9(C)**, and cut from the solid metal (usually copper). These moving charges, in turn, produce their own retarded potentials, $V_\sigma(wt)$, $\vec{A}_\sigma(wt)$ and fields, $\vec{E}_\sigma(wt)$ and $\vec{B}_\sigma(wt)$. We end up with total fields, $\vec{E}_t(wt)$ and $\vec{B}_t(wt)$, inside the magnetron space, including the cylindrical cavities (eight of them most of the time) behind the radius b. These cylindrical cavities are there, precisely, to trap microwaves in them and due to their perfect conducting walls, $\vec{E}_{tot}(wt)$ and $\vec{B}_{tot}(wt)$ reflected from them with almost no losses, and so these cavities sustain stationary microwave patterns of cylindrical geometry. The same process takes place in the eight cylindrical cavities distributed along the perimeter of radius b. With a simple wire antenna, microwaves are taken out of these cavities and sent to the entrance of the waveguide; then, these microwaves travel the short distance inside the waveguide and end up in the cooking chamber of the microwave oven; hence, our coffee absorbs so much the energy of these microwaves; the electric dipoles in the water vibrate and jiggle; frenetically, at 2.45 GHz, in a few seconds our coffee is hot and ready to drink.

11. Conclusions

In this chapter, detailed electrodynamic descriptions of the fundamental workings of microwave heating devices were given. We analyzed one by one the principal components of a microwave heater; the cooking chamber, the waveguide, and the microwave sources, either klystron or magnetron. The boundary conditions at the walls of the resonant cavity and at the interface between air and the surface of the food were stressed. It was shown how relevant the boundary conditions are to understand how the microwaves penetrate the nonconducting, electric polarizable specimen. In addition to microwave food, we mentioned the important application of microwaving waste plastics to obtain a good H_2 quantity that could be used as a clean energy source for other machines and so contributing to a cleaner planet. We did use Maxwell equations to obtain trapped stationary microwaves in the resonant cavity and traveling waves in the waveguides. We showed 3D plots of a few lower E_x, E_y, E_z modes calculated directly from the solutions obtained here and compared the general trend with experimentally obtained microwave heated patters inside rectangular cavities. The agreement is very good. We did simulate a single electro-magnetic field mode inside a cylindrical cavity in order to contrast with the stationary patterns obtained in rectangular cavities. The radiation processes in klystrons and magnetrons were stated in terms of the accelerated electrons

produced. Then, using the Lienard-Wiechert potentials produced by these electrons, the Jefimenko fields were written. When all these are put together, we understand how a meal or a waste plastic, or an industrial sample, is microwave heated.

Author details

Rafael Zamorano Ulloa
Superior School of Physics and Mathematics, IPN, Mexico City, Mexico

*Address all correspondence to: davozam@yahoo.com

IntechOpen

References

[1] Penzias AA, Wilson RW. A measurement of excess antenna temperature at 4080 Mc/s. Astrophysical Journal Letters. 1965;**142**: 419-421. DOI: 10.1086/148307

[2] Microwave Ablation 'Safe and Effective Technique' at Treating Large Benign Thyroid Nodules [Internet]. 2020. Available from: https://www.healio.com/news/endocrinology/20201020/microwave-ablation-safe-and-effective-technique-at-treating-large-benign-thyroid-nodules [Accessed: 14 March 2021]

[3] Cancer Research. Microwave Ablation. Lung Cancer [Internet]. UK: Cancer Research; 2021. Available from: https://www.cancerresearchuk.org/about-cancer/lung-cancer/treatment/microwave-ablation [Accessed: 14 March 2021]

[4] Makul N, Rattanadecho P, Pichaicherd A. Accelerated microwave curing of concrete: A design and performance related experiments. Cement and Concrete Composites. 2017; **i3**:415. DOI: 10.1016/j.cemconcomp.2017.08.007

[5] Halim SA, Swithenbank J. Simulation study of parameters influencing microwave heating of biomass. Journal of the Energy Institute. 2019;**92**:1191-1212. DOI: 10.1016/j.joei.2018.05.010

[6] Mingos M, Baghurst D. Applications of microwave dielectric heating effects to synthetic problems in chemistry. Chemical Society Reviews. 1991;**20**:1-47. DOI: 10.1039/CS9912000001

[7] Kappe O, Dallinger D. The impact of microwave synthesis on drug discovery. Nature Reviews. Drug Discovery. 2006; **54**:5. DOI: 10.1038/nrd1926

[8] Vollmer M. Physics of the microwave oven. Physics Education. 2004;**39**:74-81. DOI: 10.1088/0031-9120/39/1/006

[9] Luan D, Wang Y, Tang J, Jain D. Frequency distribution in domestic microwave ovens and its influence on heating pattern. Journal of Food Science. 2017;**82**:429-436. DOI: 10.1111/1750-3841.13587

[10] Nissinen TA, Kiros Y, Gasik M, Leskela M. $MnCo_2O_4$ preparation by microwave-assisted route synthesis (MARS) and the effect of carbon admixture. Chemistry of Materials. 2003;**15**:4974-4979

[11] Kubel E Jr. Industrial Heating. Special Focus: Advancements in Microwave Heating Technology [Internet]. 2005. Available from: https://www.industrialheating.com/articles/87800-special-focus-advancements-in-microwave-heating-technology [Accessed: 14 March 2021]

[12] Hussein MZ, Zainal Z, Ming CY. Microwave-assisted synthesis of Zn-Al-layered double hydroxide-sodium dodecyl sulfate nanocomposite. Journal of Materials Science Letters. 2000;**19**: 879-883

[13] Kay E, Gibbons KE, Jones M, Blundell SJ, Mihut A, Gameson I, et al. Rapid synthesis of colossal magnetoresistance manganites by microwave dielectric heating. Chemical Communications. 2000;**2**:159-160

[14] WiFi Wikipedia [Internet]. 2021. Available from: https://en.wikipedia.org/wiki/Wi-Fi [Accessed: 14 March 2021]

[15] Simon CJ, Dupuy DE, Mayo-Smith W. Microwave ablation: Principles and applications. Radiographics. 2005;**25**: S69-S83. DOI: 10.1148/rg.25si055501

[16] Chiu H-M, Sanagavarapu AM, Weily AR, Guy D, Ross D. Analysis of a novel expanded tip wire (ETW)

antenna for microwave ablation of cardiac arrhythmias. IEEE Transactions on Biomedical Engineering. 2003;**50**: 890

[17] Roy R, Peelamedu R, Grimes C, Cheng J, Agrawal D. Major phase transformations and magnetic property changes caused by electromagnetic fields at microwave frequencies. Journal of Materials Research. 2002;**17**:3008-3011

[18] Makul N, Rattanadecho P. Microwave pre-curing of natural rubber-compounding using a rectangular waveguide. International Communications in Heat and Mass Transfer. 2010;**37**:914-923. DOI: 10.1016/j.icheatmasstransfer.2010.03.001

[19] Villegas RV. Non-linear physics of magnetization under microwave and Zeeman excitation in ferromagnetic materials (Física no-lineal de la magnetización bajo excitación Zeeman y de microondas en materiales ferromagnéticos) [doctoral thesis]. Mexico: Instituto Politécnico Nacional; 2019

[20] Microwaving Plastic Waste Can Generate Clean Hydrogen [Internet]. 2021. Available from: https://www.newscientist.com/article/2256822-microwaving-plastic-waste-can-generate-clean-hydrogen/#::text=Chemists%20have%20used%20microwaves%20to,developed%20to%20transform%20the%20plastic [Accessed: 14 March 2021]

[21] Jie X. Microwave initiated catalytic deconstruction of plastic waste into hydrogen. Nature Catalysis. 2020;**3**: 902-912. DOI: 10.1038/s41929-020-00518-5

[22] Booth K. £20M Plastic to Hydrogen Plant at Peel L&Ps Protos Moves Forward, Building-Design & Construction Magazine (BDC). Trafford City, Manchester, UK: Peel (L&P) UK; 2020

[23] Uekert T, Kuehnel M, Wakerley DW, Reisner E. Plastic waste as a feedstock for solar driven H_2 generation. Energy & Environmental Science. 2018;**11**:2853-2857. DOI: 10.1039/C8EE14K408F

[24] Feynman RP, Leighton RB, Sands M. The Feynman Lectures on Physics. Mainly Electromagnetism and Matter. Vol. II. The New Millennium Edition. New York: Basic Books; 2010. p. 566. ISBN: 978-0-465-07998-8

[25] Lorain P, Corson D. Electromagnetic Fields and Waves. 2nd ed. New York: WH Freeman and Company; 1970. p. 696. ISBN: 0-7167-0331-9

[26] Jackson JD. Classical Electrodynamics. New York, London: John Wiley & Sons, Inc.; 1962. p. 656

[27] Griffiths DJ. Introduction to Electrodynamics. 3rd ed. New Jersey, USA: Prentice Hall; 1999. p. 576

[28] Wangsness RK. Electromagnetic Fields. New York, London: John Wiley; 1986. p. 286

[29] Reitz JR, Milford FJ, Christy RW. Foundations of Electromagnetic Theory. 4th ed. Reading, Massachusetts, USA: Adison-Wesley; 2008. p. 345. ISBN: 10-0321581747

[30] Kamol S. Three-dimensional standing waves in a microwave oven. American Journal of Physics. 2010;**78**: 492-495. DOI: 10.1119/1.3329286

[31] Steyn-Ross A. Standing waves in a microwave oven. The Physics Teacher. 1990;**28**:474-476. DOI: 10.1119/1.2343114

[32] Jefimenko OD. Electricity and Magnetism: An Introduction to the Theory of Electric and Magnetic Fields. 2nd ed. New York: Appleton-Century-Crofts; 1966. ISBN: 978-0-917406-08-9